Arabian Journal of Chemistry (2023) **16**, 104439

King Saud University

Arabian Journal of Chemistry

www.ksu.edu.sa
www.sciencedirect.com

ORIGINAL ARTICLE

Effective adsorption of Hg(II) ions by new ethylene imine polymer/β-cyclodextrin crosslinked functionalized magnetic composite

Wei Long [a,b,*], Chengyue Yang [c], Gongshu Wang [c], Jianshe Hu [c,*]

[a] *Guangdong Provincial Key Laboratory of Petrochemical Pollution Process and Control, Guangdong University of Petrochemical Technology, Maoming 525000, People's Republic of China*
[b] *College of chemistry, Guangdong University of Petrochemical Technology, Maoming 525000, People's Republic of China*
[c] *Center for Molecular Science and Engineering, College of Science, Northeastern University, Shenyang 110819, People's Republic of China*

Received 3 August 2022; accepted 13 November 2022
Available online 19 November 2022

KEYWORDS

β-cyclodextrin;
Hg(II) ions;
Ethylene imine polymer;
Adsorption;
Magnetic composite nanomaterial

Abstract A new effective magnetic composite material was prepared successfully for adsorption Hg(II) ions by introducing β-cyclodextrin/ethylene imine polymer to the mesoporous silica. The morphology and structure of EIP-β-CD magnetic adsorbents were characterized by FT-IR, XR, DTG, XPS and SEM technologies. The effect of many factors were discussed detailedly such as adsorption time, initial concentration, pH, different composition of adsorbent and adsorption temperature. It was found that EIP-β-CD showed excellent adsorption capacity, high selectivity, good reutilization and fast adsorption rate. The maximum adsorption capacity was 248.72 mg/g and the best removal rate was 99.49 % under the optimized experimental conditions. The kinetic and thermodynamic study showed typical characteristic of chemical adsorption, exothermic and spontaneous. The best mass proportion of β-cyclodextrin, ethylene imine polymer and glutaraldehyde was 1.0:0.4:0.2, and proper β-cyclodextrin can develop the adsorption capacity for Hg(II) ions in this adsorbent. The possible adsorption mechanism was investigated in detail. After the fifth cycle experiment, this new adsorbent still showed excellent adsorption capacity which indicated that it has great potential for Hg(II) ions cleanup in water solution.

* Corresponding authors.
E-mail addresses: longwei@gdupt.edu.cn (W. Long), hujs@mail.neu.edu.cn (J. Hu).
Peer review under responsibility of King Saud University.

Production and hosting by Elsevier

https://doi.org/10.1016/j.arabjc.2022.104439
1878-5352

1. Introduction

As the rapid growth in technologies and industries, many heavy metals pollution in the environment were more and more serious (Rivas et al., 2012). Particularly, mercury has high toxicity, non-biodegradability and bio accumulation, which was listed in the top ten chemicals of public concern by the World Health Organization (WHO) (Kingston, 2020). Mercury can bio-accumulate in food chains, form mercury organic compounds in human body and ultimately accumulates, so mercury is a high dangerous element and it's removal process is very difficult (Dziok et al., 2020).

Mercury pollution was a global and devastating threat to human health and the environment, and about 11,000 tons/year industrial wastewater containing Hg(II) ions was discharged(Boening, 2000). Many species containing mercury were found in the garbage or municipal wastes derived from oil refinery, coal combustion, color-alkali production, pharmaceutical, paint production, ferrous metallurgy and metal mining (Gallup et al., 2017) Both Hg^0 in the contaminating atmosphere and Hg^{2+} ions in aqueous solutions are not friendship to human health (She et al., 2020; Girginova et al., 2010). When the mercury was accumulated in the human body, serious diseases may break out and can not be cured, especially as Alzheimer (Pigatto et al., 2018) or Parkinson's Disease (Ullah et al., 2021).

So, it is urgent to eliminate mercury from the gas or wastewater before it is released into the environment (Ma et al., 2011). Many methods as ion exchange (Chiarle et al., 2000), membrane separation (Tian et al., 2011), adsorption (Park et al., 2018) and precipitation (Wang et al., 2018) were employed to remove mercury in gas phase or liquid phase. Among them, adsorption is applied widely due to its advantages of fast action, flexibility, superior removal efficiency, low energy consumption, low operating costs and easy access to raw materials (Guo et al., 2020).

The different adsorbents exhibited different adsorption capacity for mercury, and many vary adsorbents were reported for good adsorption of Hg2+(Bibby and Mercier, 2002; Clercq, 2012; Forbes, 1974; Saeed et al., 1999; Somayajula et al., 2013; Zhang et al., 2009; Mo and Lian, 2010). The adsorption of the Hg(II) ions started at 1974 year, and hydroxyl amount on the surface of the adsorbent was the important factor (Forbes, 1974). Typical; Saeed et al investigated the formation of Hg(II)-SCN complex in the adsorption process, 0.1 mol/L hydrochloric acid solution was best solvent (Saeed et al., 1999). A chelating ion exchange resin named Duolite GT-73 with thiol groups was synthesized successfully and applied for Hg(II) ions removal. Chirle et al (Wang et al., 2018) found the adsorption speed controlling step was intraparticle diffusion. Bibby et al (Bibby and Mercier, 2002) proposed Thiol-Functionalized mesoporous silica microspheres could be used for Hg^{2+} adsorption and an new ion permeation and displacement mechanism was proposed. SH-ePMO, TP-214, low-cost activated carbon, bacillus mucilaginosus and silica-gel were reported for adsorption of Hg(II) ions (Clercq, 2012; Somayajula et al., 2013; Zhang et al., 2009; Mo and Lian, 2010), and the asdorption capacity depended on the functional groups.

Nowadays, some polymer materials exhibited great advantage for the adsorption aspect. Zhou et al (Zhou et al., 2009) prepared thiourea-modified magnetic chitosan material; and the maximum adsorption capacity was 625.0 mg/g for Hg^{2+} ions. He found that Hg^{2+} ions can be adsorbed selectively in solution containing many other metal ions by ehylenediamine-modified magnetic crosslinking chitosan microsphere, and the removal rate of Hg^{2+} ions was more than 90 % (Zhou et al., 2010). Polyaniline/humic acid composite was applied for the adsorption of Hg(II) and Cr(VI) ions at the same time, and the maximum adsorption capacity of Hg(II) ions was 672.0 mg/g (Li et al., 2011). Wang et al prepared chitosan-poly(vinyl alcohol)/bentonite composite material, and the best adsorption capacity for Hg(II) ions was 460.18 mg/g (Wang et al., 2014). Another kind of functionalized magnetic composite material of tannic acid cross-linking cellulose/polyethyl eneimine was prepared successfully, and its adsorption capacity for Hg(II) ions reached 247.51 mg/g (Sun et al., 2021). Hence, magnetic polymer composite materials exhibited great potential adsorption capacity for Hg(II) ions, but the preparation process was complicated.

Another important factor of the effective adsorbent is the monomer or ligand of polymerization, organic monomer which contains a variety of groups maybe show special adsorption capacity. β-cyclodextrin (β-CD) was reported as good organic ligand in the adsorbent, which contained an apolar cavity with two kinds of hydroxyl groups (inside and outside) (Szejtli, 1998). β-CD can be introduced into adsorbent forming functionalized composite materials by crosslinking reaction, which can adsorb many pollutants as Cu(II) ions (Badruddoza et al., 2011); methylene blue (Yang et al., 2016), and methyl orange (Yan et al., 2016) effectively. The crosslinking reaction can be effected by the ratio of reactants, reaction temperature, crosslinking agents and cross-linking time (Monrin-Crini and Crini, 2013). Gawish et al used citric acid as a cross-linking agent for grafting β-CD onto wool fabric and better antimicrobial property was detected (Gawish et al., 2009). Glutaraldehyde was a good cross-linking agent for the synthesis of cross-linked cyclodextrin polymer materials (Mohamed et al., 2012). The cross-linked structure of the polymer can be controlled effectively by varying the amount of cross-linking agent, and the cross-linking density can determine the special performance (Hoti et al., 2021). Hence, the removal of heavy metal ions also can be realized by novel functional polymer composite materials containing β-cyclodextrin by crosslinking reaction.

In order to exposit the advantage and potential capacity of novel magnetic β-cyclodextrin polymer composite material for the removal of Hg(II) ions, EIP-β-CD was prepared successfully based on ethylene imine polymer and β-cyclodextrin as raw materials. Its adsorption performance in the removal of Hg(II) ions was investigated in detail consider the different conditions, the results were good due to many active groups on the surface of adsorbent. The introduction of β-cyclodextrin could develop the adsorption capacity of adsorbent effectively, and the reutilizate performance of EIP-β-CD adsorbent was good. Moreover, the equilibrium data was analyzed carefully by Langmuir and Freundlich isotherm models (Fu et al., 2021), which based on our previous research. The best mass proportion of β-cyclodextrin, ethylene imine polymer and glutaraldehyde was found, and the adsorption for Hg (II) ions by this adsorbent was independent of the interfering anions. The adsorption kinetics and adsorption mechanism were investigated in detail, so this special function of EIP-β-CD adsorbent was revealed successfully. Hence, as the efficient, practical, and novel magnetic polymer composite material, EIP-β-CD adsorbent exhibited great advantage for the removal Hg(II) ions in water solution, and which could be used to selectivity for Hg(II) ions cleanup. All these works played an important guiding significance for the removal of Hg(II) ions.

2. Materials and methods

2.1. Materials

Nano ferric oxide, tetraethoxysilane (TEOS), Triton X-100, 3-aminopropyltriethoxy silicon (APTES) and glutaraldehyde were purchased from Sinopharm Chemical Reagent Co., ltd. Dimethyl sulfoxide (DMSO), anhydrous ethanol, ammonia water, ammonium nitrate, hydrochloric acid, nitric acid, sodium hydroxide and pyridine were purchased from Tianjin Damao Chemical Reagent Co., ltd. Cetyltrimethyl bromide (CTAB) was provided by Shanghai McLean Biochemical Technology Co., ltd. Dithizone, ethylene imine polymer (25 %) and β-cyclodextrin was purchased from NanJing Chemical Reagent Corporation Limited Co., ltd. Mercury nitrate was purchased from Guangzhou ZeHui Environmental Science and Technology Co., ltd.

2.2. Preparation of EIP-β-CD

2.2.1. Preparation of Fe_3O_4@SiO_2

In order to purify the nano ferric oxide, Fe_3O_4 (2.0 g) was dispersed in HCl solution (0.25 mol/L, 250 mL) and stirred continuously for 3 h. Nano Fe_3O_4 was separated with magnet, and further washed with distilled water some times. Next, the nano Fe_3O_4 (1.0 g) was dispersed in a round flask with 40 mL distilled water, 160 mL ethanol, 10 mL ammonia water and a certain amount of TEOS were added into the mixture carefully, continuously stirred for 12 h (Sun et al., 2021; Yang et al., 2021). After the solid was separated with magent, it was washed some times by distilled water, then dried in an oven and labled as Fe_3O_4@SiO_2.

2.2.2. Preparation of Fe_3O_4@SiO_2@SiO_2

According to the similar prepared method in literature (Sun et al., 2021; Yang et al., 2021); Fe_3O_4@SiO_2 (1.0 g) was dispersed in a mixture of CTAB (0.1 g), anhydrous ethanol (400 mL), and distilled water (140 mL) under vigorous stirring. 20 mL TEOS was added slowly to the mixed solution and was stirred for 10 h at 75 °C. Then, the powder was separated with magnet and washed with distilled water some times, the powder was vacuum dried at 60 °C for 5 h. Consider the residual CTAB constituent, the powder was redispersed in ethanol solution and ammonium nitrate (0.50 g) was added, then the mixture solution was refluxed for 8 h at 85 °C. The product was collected magnetically again and washed by distilled water several times, then dried in a vacuum for 8 h at 55 °C. So the nano Fe_3O_4@SiO_2@SiO_2 was obtained and it was named as MMS.

2.2.3. Preparation of MMS-NH_2

Typical, 1.0 g of the MMS powder was redispersed in 80 mL of pyridine, 2.0 mL of ammonia water and 1.0 mL of APTES were added into the mixture carefully. The mixture solution was stirred for 12 h with the protection of N_2 atmosphere. The brown powder was collected magnetically again and washed by distilled water some times, then it was dried in a vacuum for 10 h at 55 °C and labled as MMS-NH_2 (Sun et al., 2021; Yang et al., 2021).

2.2.4. Preparation of EIP-β-CD

Some β-cyclodextrin solid was dissolved in DMSO solvent carefully, the mixture was stirred at 55 °C in flask under the protection of N_2 atmosphere. Then, 1.0 mL of APTES were dropped into the flask slowly and stirred at 55 °C for 3 h. Some ethylene imine polymer (25 %) was added in DMSO and stirred 30 min to form a uniform solution in another flask at room temperature. Then, some ethylene imine polymer solution, some β-cyclodextrin solution, MMS-NH_2 solid and DMSO were added into a flask. After ultrasonic dispersion for 15 min, glutaraldehyde was dropped into the mixture slowly and was stirred quickly and refluxed at 85 °C for 10 h under the protection of N_2 atmosphere. After cooled to the room temperature, the red powder was washed with distilled water and vacuum dried for 8 h at 55 °C to obtain a magnetic ethylene imine polymer/β-cyclodextrin composite material (EIP-β-CD). Fig. 1 describes schematic illustration of the preparation of the EIP-β-CD adsorbent.

2.3. Characterization

Powder X-ray diffraction (XRD) patterns were determined under a D/max 2500 TC diffractometer using Cu-Kα radiation (λ = 1.541 A) at 40 kV and 35 mA between 10 and 80°(2θ). Fourier transform infrared (FT-IR) spectra of the samples were recorded as the KBr films in the range of 500–4000 cm^{-1} on a Nicolet 380 spectrometer. A vibrating-sample magnetometer (VSM) were recorded on a EG & G Princeton Applied Research Vibrating Sample Magnetometer. The morphology of the samples were observed by scanning electron microscope (SEM, JEOL 6500F). The BET characterization of the samples were performed ony the nitrogen adsorption–desorption on a Quantachrome NOVA-2210e automated gas sorption system and the results were calculated by Brunauer-Emmett-Teller(BET) and Barrett-Joyner-Halenda(BJH) methods. X-ray photoelectron spectroscopy (XPS) were recorded with a Perkin Elmer EHI5000C ESCA system equipped with a hemispherica electron energy analyzer. TG curves of the samples were recorded by a TGA/DCS using nitrogen atmosphere as purge gas (40 mL/min) over a temperature range of 50 ~ 800 °C and with a heating rate of 10 °C/min.

2.4. Adsorption and desorption research

EIP-β-CD as the adsorbent, it is applied for mercury(II) ions adsorption process. Many influencing factors as initial Hg(II) ions concentration, adsorption time, the pH of solution and temperature were investigated in detail. 1000 mg/L standard Hg(II) ions solution was configured by dissolving $Hg(NO_3)_2$ solid carefully, lots of lower standard Hg(II) ions solutions were configured by diluting this solution with distilled water, the certain pH value was adjusted by the addition of HNO_3 or NaOH solutions slowly. The changed of pH value (ΔpH) in every experiment was very small, and this parameter can be ignored.

For investigating the effect of the initial Hg(II) ions concentration, 0.01 g of EIP-β-CD powder as the adsorbent was added into the 50 mL solutions with the different Hg(II) ions concentration from 50 mg/L to 300 mg/L, and pH value of all solutions was 5.0 and adsorption time was fixed at 180 min at 293 K. The conditions of investigating the effect of adsorption time: EIP-β-CD adsorbent, 0.01 g; initial Hg(II) ions concentration, 50 mg/L; solution volume, 50 mL; temperature, 293 K, pH, 5.0. The conditions of investigating the effect of adsorption temperature: EIP-β-CD adsorbent, 0.01 g; initial Hg(II) ions concentration, 50 mg/L; solution volume, 50 mL; pH, 5.0; adsorption time, 180 min. The conditions of investigating the influence of coexisting ions: EIP-β-CD adsorbent, 0.01 g; initial Hg(II) ions concentration, 50 mg/L; solution volume, 50 mL; pH, 5.0; adsorption time, 180 min; temperature, 293 K; Na(I), K(I), Mg(II), Al(III) and Ca(II) ions concentration, 50 mg/L.

After adsorption experiment, the remaining Hg(II) ions concentration was analyzed by the national standard colorimetric method (GB/T5750.6–2006). The adsorption capacity or adsorption efficiency are calculated by the following equations.

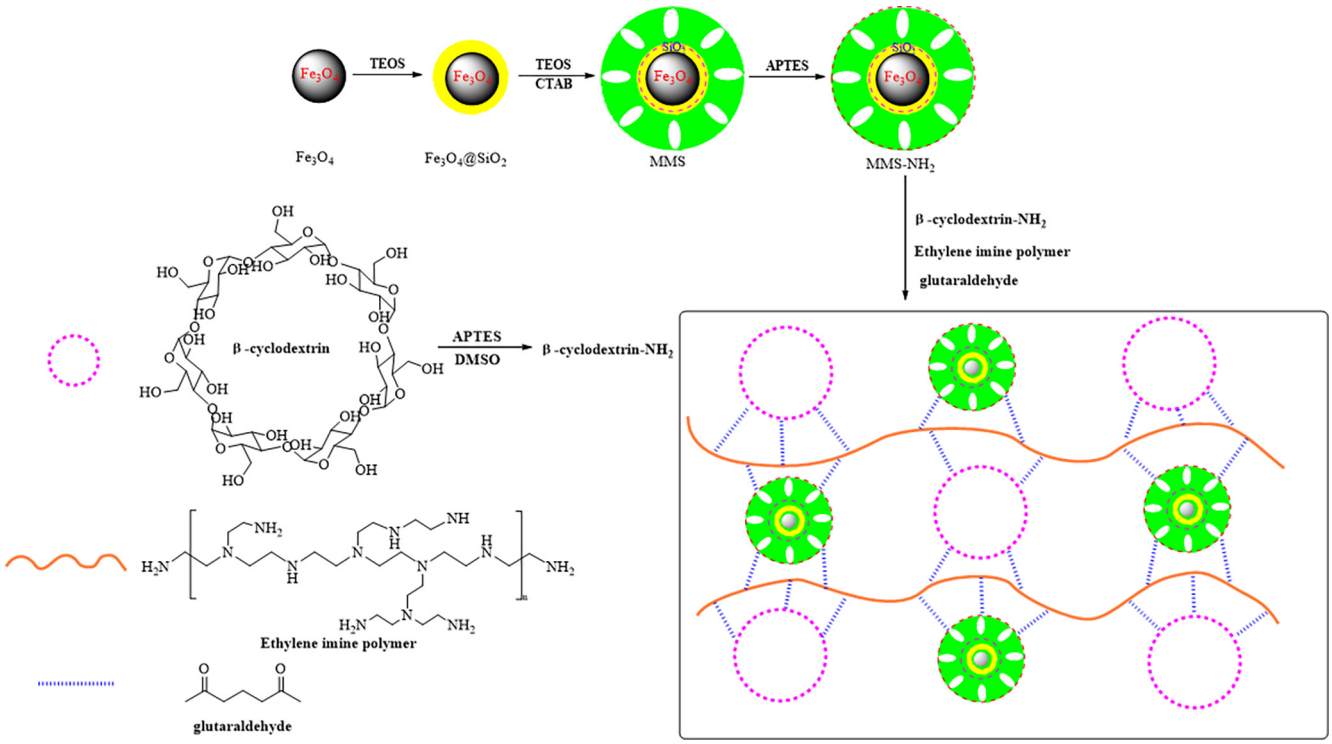

Fig. 1 Schematic illustration of the preparation of the EIP-β-CD.

$$Q_e = \frac{(C_0 - C_e) \times V}{m} \quad (1)$$

$$R = \frac{(C_o - C_e)}{C_0} \times 100\% \quad (2)$$

Where Q_e (mg/g) represents the adsorption capacity of adsorbent for Hg(II) ions in water solution; C_0 represents the initial Hg(II) ions concentration (mg/L) before adsorption; C_e represents the equilibratory Hg(II) ions concentration (mg/L) after adsorption; m represents the substrate mass (g) of adsorbent and V represents the solution volume (L); R represents the removal efficiency (%) of Hg(II) ions.

Additional, for the desorption experiment, 0.01 g of EIP-β-CD adsorbent was added into 50 mL of mercury(II) ions solution (50 mg/L) at 293 K, pH 5 and stirred for 180 min. Then the Hg(II)-adsorbed EIP-β-CD was collected from the water solution and it was transfered into HCl solution (3 mol/L) for desorption experiment (Sun et al., 2021; Yang et al., 2021). Next, the desorbed EIP-β-CD powder was washed with distilled water some times and vacuum dried for 8 h at 55 °C. It was reused carefully for the reutilization performance research at the same condition, which was consisted with our previous research (Yang et al., 2021).

3. Results and discussion

3.1. Characterization of EIP-β-CD

3.1.1. FT-IR analysis

FT-IR characterization is applied to distinguish the chemical composition of MMS-NH_2, β-CD and EIP-β-CD. According to the alone signal of β-CD sample, some broad adsorption peaks between 1028 cm^{-1} to 1180 cm^{-1} are belonged to the stretching vibration of C—O at inner site of β-CD molecule in Fig. 2**(a)**. There are also small weak peaks at 1409 cm^{-1} and 1439 cm^{-1} due to the stretching vibration of C—O—C bond or many hydroxyl. There are some small adsorption peaks near 1421 cm^{-1} due to the distorte vibration of –CH_2– of β-CD molecule. A sharpen peak at 1647 cm^{-1} is belonged to the intramolecular hydrogen bond of β-CD molecule. A distinct adsorption peak at 2927 cm^{-1} due to the stretching vibration of –CH_2– in β-CD molecule. There are many broad adsorption peaks near 3390 cm^{-1} are belonged to the stretching vibration of hydroxyls in β-CD molecule (Yan et al., 2016).

For the MMS-NH_2 sample, there is a broad peak near 550 cm^{-1} is belonged to the oscillation of Fe-O bond (Ghasemzadeh et al., 2015). A strong characteristic adsorption peak near 799 cm^{-1} and the absorption peak near 1089 cm^{-1} are belonged to the symmetric and antisymmetric stretching of Si-O-Si bond, respectively (Yilmaz et al., 2017). A smal peak near 1402 cm^{-1} is belonged to the antisymmetric stretching vibration of –CH_2– in APTES molecule. The weak peak near 1630 cm^{-1} and broad peak near 3348 cm^{-1} are belonged to the vibration of amino groups (Zhou et al., 2017). Hence, –NH_2 groups was grafted to the surface of MMS particles successfully.

The all characteristic peaks of β-CD and MMS-NH_2 are displayed for the EIP-β-CD sample in Fig. 2**(a)**, and there is a little red shift for the EIP-β-CD sample clearly. Two new peaks are displayed near 1091 cm^{-1} are the characteristic absorption peaks of C—N and N—H bond due to the introduction of ethylene imine polymer (Yuan et al., 2014). Some clear adsorption peaks at 1355, 1412 and 1465 cm^{-1} are belonged to the different vibration of –NH_2. Additional, new absorption peaks near 2850 cm^{-1} or 2983 cm^{-1} for EIP-β-CD sample

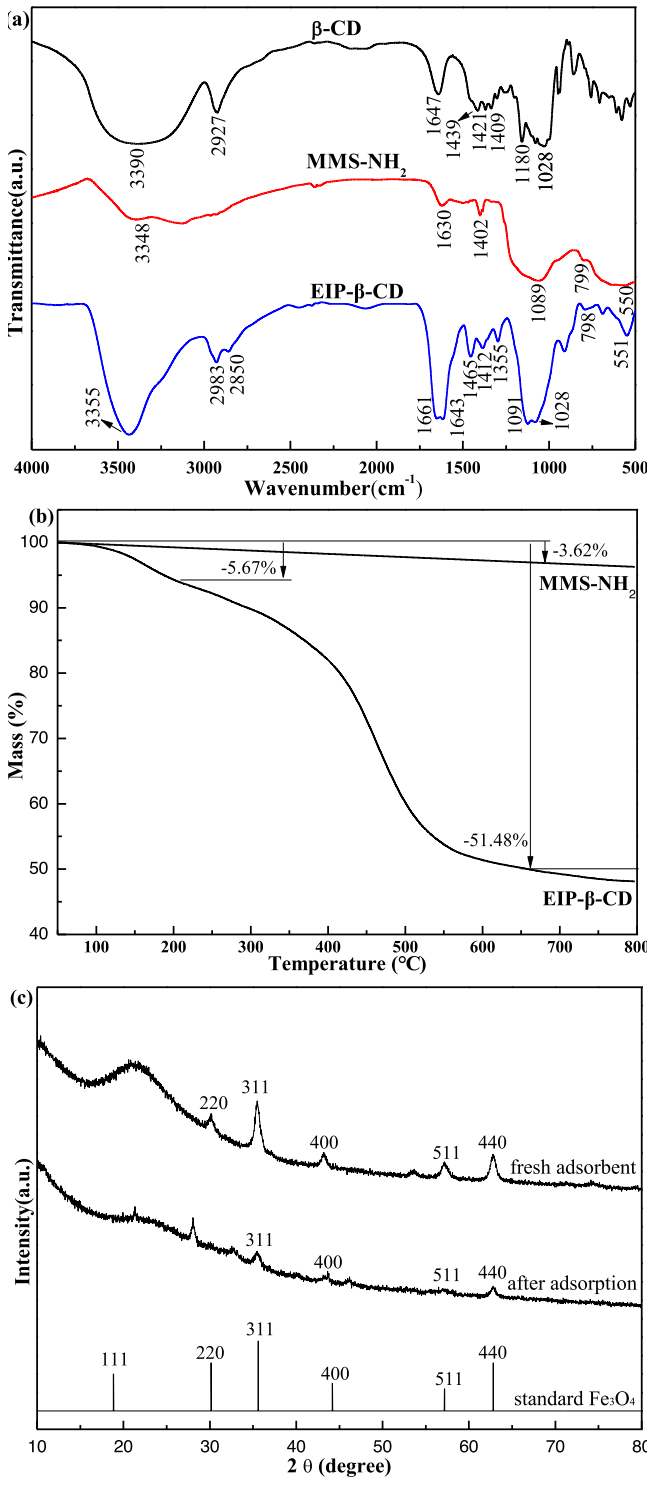

Fig. 2 (a) FT-IR spectra of β-CD, MMS-NH_2 and EIP-β-CD; (b) TG curves of EIP-β-CD and MMS-NH_2; (c) XRD patterns of EIP-β-CD and standard Fe_3O_4; (d) VSM analysis of EIP-β-CD; (e) Nitrogen adsorption desorption loop and BJH pore size distribution analysis of EIP-β-CD.

are belonged to the symmetric or asymmetric stretching vibrations of $–CH_2$ group. This indicate that the ethylene imine polymer and β-CD are grafted on the surface of magnetic particles successfully.

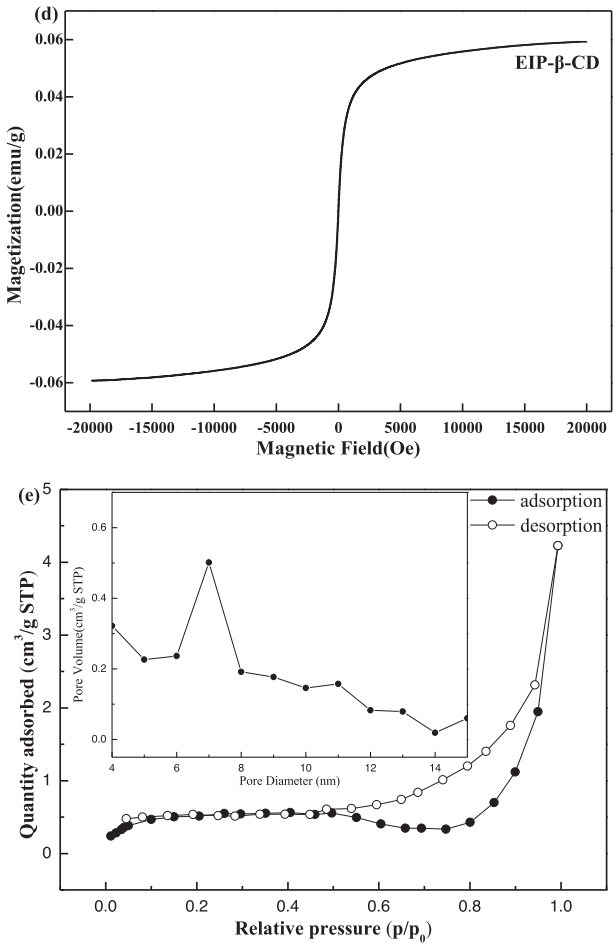

Fig. 2 (*continued*)

3.1.2. TG analysis

The curves of EIP-β-CD and MMS-NH_2 are displayed in Fig. 2**(b)**. For the first decomposition stage (50–190 °C) of EIP-β-CD particles, the weight loss rate is approx. 5.67 % is attributed to the loss process of physisorbed water and part of the hydroxyl (–OH) groups. For the second stage (200–660 °C), the distinct weight loss rate is approx. 45.81 % is attributed to the decomposition of β-CD molecule and ethylene imine polymer (Yan et al., 2016); so the thermodynamic properties of EIP-β-CD is not stable. While from Fig. 2**(b)**, the weight loss rate is approx. 3.62 % from the TG curve of MMS-NH_2 particles, which suggest that good thermal stability and both $–NH_2$ and mesoporous silica were coated onto the micro Fe_3O_4 particles.

3.1.3. XRD characterization

XRD patterns of EIP-β-CD particles are displayed in Fig. 2**(c)**. As is shown from Fig. 2**(c)**, XRD patterns of fresh adsorbent show the typical characteristic of standard Fe_3O_4(No.65–3017) (Phothitontimongkol et al., 2009), orderly structure and crystallization are approved for the EIP-β-CD particles due to the existence of broad distinct diffraction peak at $2\theta = 21.3°$. It can be seen that adsorbent appears some dispersive diffraction peaks near $2\theta = 22.0°$ after adsorption from

Fig. 2**(c)**. The reasons maybe are the disorder of crystal structure increasing and the integrity of crystal structure is lower significantly after adsorption (Pouya et al., 2020). The distinct diffraction peak appears near 2θ = 28.3° is attributed to the strong interaction between many active hydroxyl groups of β-CD molecule with Hg(II) ions in solution. The other diffraction peaks are similar in Fig. 2**(c)**.

3.1.4. VSM characterization

The VSM curve of the EIP-β-CD adsorbent is displayed in Fig. 2**(d)**. The magnetization saturation (Ms) of EIP-β-CD adsorbent is 0.06 emu/g from the Fig. 2**(d)**, and this lower value is attributed to the surface coating of polymers and SiO_2, but this weak magnetic property can satisfy fast adsorption and fast separation.

3.1.5. BET analysis

Nitrogen adsorption desorption loop and BJH pore size distribution analysis for the EIP-β-CD adsorbent are shown in Fig. 2**(e)**. According to the IUPAC classification, it can be seen that the EIP-β-CD absorb is of type IV, a hysteresis loop with distinct weak platform at the site of the moderate relative pressure, so the pores are ordered highly. This reslut exhibits the feature of mesoporous structure, and the pore diameter distribution of this adsorbent are focused at 7.1 nm in Fig. 2**(e).** Additional, the surface area and pore volume of the EIP-β-CD absorbent are 6.684 m^2/g and 0.115 m^3/g, respectively.

3.1.6. SEM characterization

SEM images of EIP-β-CD adsorbent and element distribution ratio are shown in Fig. 3. The surface of EIP-β-CD (Fig. 3**(a)**) is not relative denser and coarse, so the ligand and the magnetic particles are crosslinked tightly with many ligands, so this magnetic composite adsorbent are prepared succefffully. Compared with SEM images of Fe_3O_4@SiO_2 and MMS-NH_2 particles in the literature (Ahmadi et al., 2017; Yang et al., 2021), the surface structure exhibits alveolate state and more thickly. The element distributions are uniform on the surface of EIP-β-CD adsorbent which are displayed clearly in Fig. 3**(b)**, C, N, O and Fe element are distributed widely on the surface of EIP-β-CD adsorbent. The different element ratio of C, N, O, Fe, Si and Au elements are shown in Fig. 3, and the content of O and Si are the major(H element is not distinguished by this method). Au element is extra added in the preparation and testing process of sample, and the accuracy element content analysis for the mapping image are listed in Table 1.

On the surface of EIP-β-CD adsorbent, carbon atomic percentage is the maximum as 49.07 % which indicate that the β-cyclodextrin and ethylene imine polymer molecules are crosslinked with the ligands on the magnetic particles. The atomic rate between O and Fe is far more than 4:3 due to the β-cyclodextrin afford many oxygen atoms. The similar case is displayed in mass percentage, and the mass percentage of Fe element is high as 25.37 % and magnetic capacity of the adsorbent material is apparent.

3.2. Effect of pH value on adsorption

In water solution, the pH value is the important parameter, and the metal ions adsorption behavior on the adsorbent surface only localize at certain pH value range. The adsorption performance of Hg(II) ions by the EIP-β-CD adsorbent (the mass proportion of β-cyclodextrin, ethylene imine polymer and glutaraldehyde is 1.0:0.4:0.2) in different pH solution (from 1 to 7) is displayed in Fig. 4. The adsorption capacity of Hg(II) ions increased as the increment of pH value from 1 to 5, but the Zeta potential value of solution decreased distinctly, and the maximum adsorption capacity appears at pH of 5. In high concentration of H^+ solution, both Hg(II) ions and H^+ automatic occupy the binding site on the surface of adsorbent at the same time, so electrostatic repulsion can decrease the formation of Hg(II) ions coordination compound.

Another explanation is amino groups on the surface of EIP-β-CD absorbent are protonated to be $-NH_3^+$ easily in high concentration of H^+ solution, so the chelating reaction become more difficulty after electrostatic repulsion. The Zeta potential value of solution is decreased with the decrement of the H^+ concentration, so the electrostatic repulsion is reduced, and the adsorption capacity of adsorbent is developed distinctly. In low concentration of H^+ solution, hydrogen ions of the hydroxyl groups tend to losing easily, so the formation of Hg(II) ions coordination complex is difficult and the adsorption capacity of adsorbent become lower. As soon as the pH value exceeds 5.0, the hydrolysis reaction of Hg(II) ions is easy to occur (pK_{sp}: $Hg(OH)_2$ = 25.51). Many hydroxides as $Hg(OH)^+$ or $Hg(OH)_2$ are generated easily by hydrolysis reaction in the weak acidic or alkaline solution (Chandra and Kim, 2011; Pourshirband and Nezamzadeh-Ejhieh, 2020). Such precipitates in solution also block the pore structure, so the adsorption capacity of this adsorbent become lower. Therefore, the optimal pH value as 5.0 is fixed as the important parameter in the further investigation.

3.3. Effect of initial Hg(II) ions concentration

The effect of initial concentration of Hg(II) ions (C_0) is another important parameter for this adsorption, and the adsorption capacity of the EIP-β-CD adsorbent (the mass proportion of β-cyclodextrin, ethylene imine polymer and glutaraldehyde is 1.0:0.4:0.2) are described with the range from 50 to 300 mg/L in Fig. 5. The initial Hg(II) ions concentration changes from 50 to 200 mg/L, the adsorption capacity of the EIP-β-CD adsorbent is developed greatly. The amount of Hg (II) ions adsorbed using the EIP-β-CD adsorbent tends to stabilize since the initial concentration of Hg(II) ions exceeds 200 mg/L.

In low concentration of Hg(II) ions solution, there are much high active sites on the surface of the EIP-β-CD adsorbent, which are more than the amount of initial Hg(II) ions in the solution, so the collision between Hg(II) ions and active sites increase inevitably, and the adsorption capacity of the EIP-β-CD adsorbent increases distinctly. In high concentration of Hg(II) ions solution, the amount of active sites on the surface of the EIP-β-CD adsorbent are not adequate. It is difficult to adsorb so much Hg(II) ions in the solution, so the curve tends to stabilize.

3.4. Adsorption isotherm analysis

In order to explore the adsorption essence and characteristic of the EIP-β-CD adsorbent (the mass proportion of β-

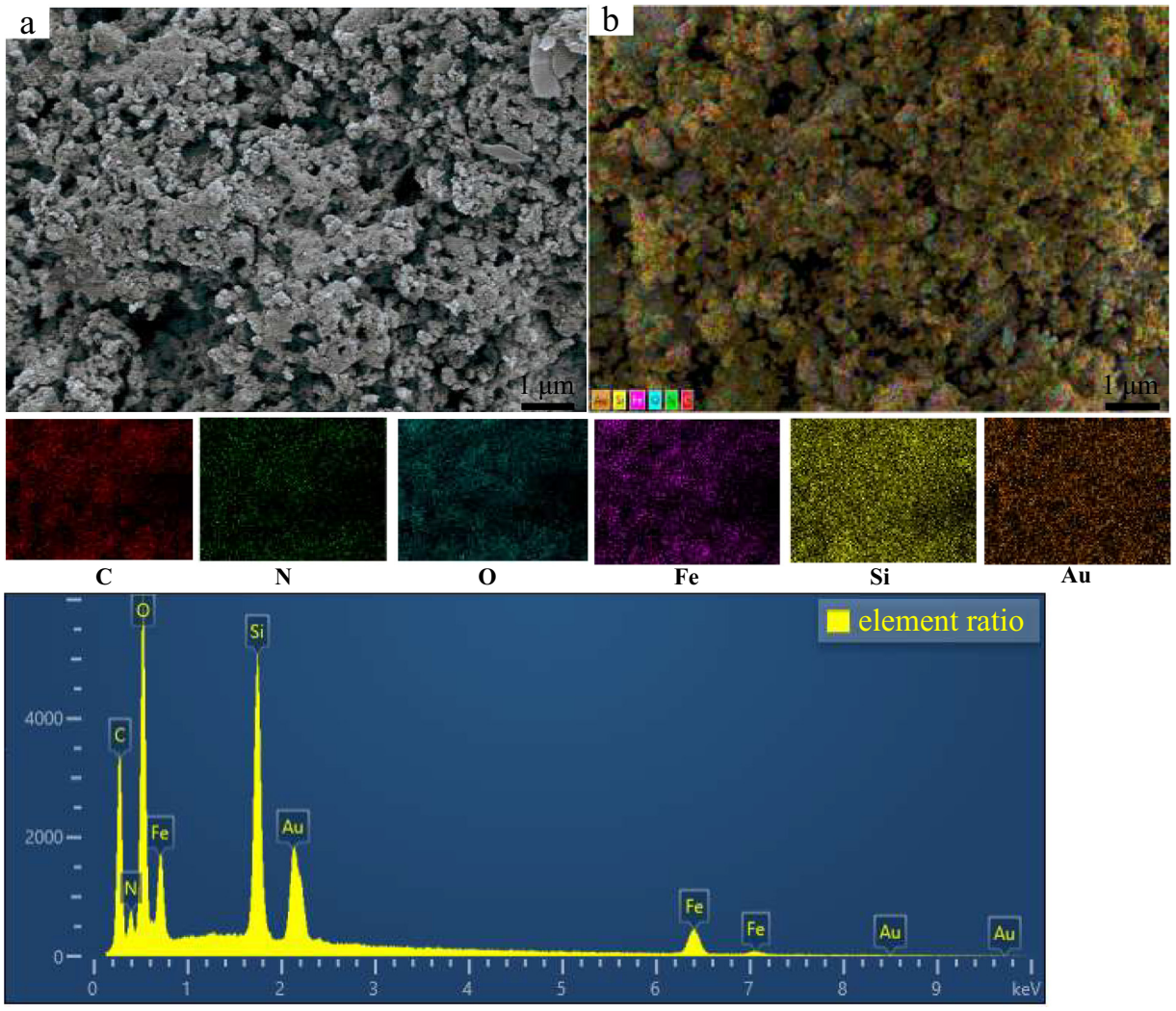

Fig. 3 SEM images of the EIP-β-CD adsorbent and element distribution ratio. (a.SEM images. b.Color element distribution images.).

Table 1 The surface element analysis of the EIP-β-CD adsorbent.

Element	Atomic percentage (%)	Mass percentage (%)
C	49.07	33.05
N	9.09	7.14
O	27.57	24.73
Fe	8.10	25.37
Si	6.17	9.71
Total	100.00	100.00

cyclodextrin, ethylene imine polymer and glutaraldehyde is 1.0:0.4:0.2) in detail, Langmuir and Freundlich isotherm models are used to investigate this adsorption behavior when the adsorption attain dynamic equilibrium (Dada et al., 2012; Fu et al., 2019). The adsorption data were fitted and evaluated carefully base on the experimental results with the different initial concentration of Hg(II) ions, and the accurate relationship between Hg(II) ions and adsorbents (the mass proportion of β-cyclodextrin, ethylene imine polymer and glutaraldehyde is

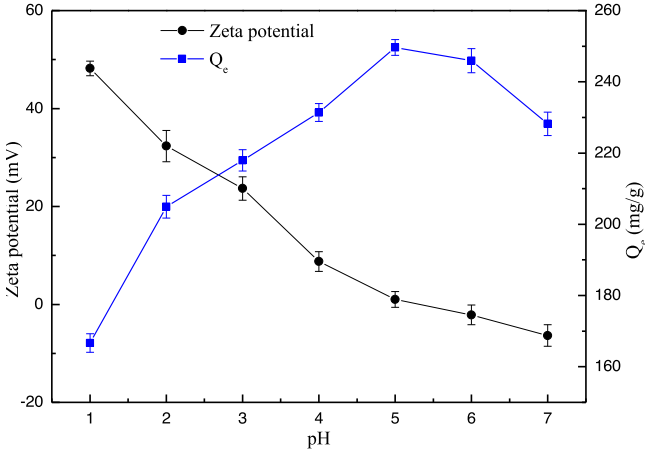

Fig. 4 Effect of pH on the sorption of Hg(II) ions.

1.0:0.4:0.2) was revealed successfully. The linear form equations of Langmuir and Freundlich models are described as follows (Ho et al., 2002; Weber and Morris, 1963).

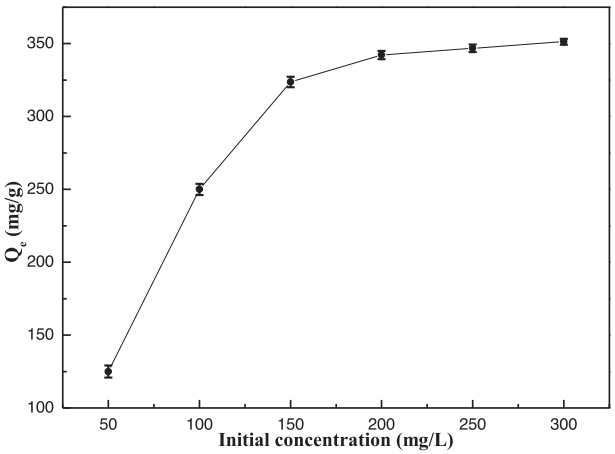

Fig. 5 Effect of initial Hg(II) ions concentration in solution on the sorption.

$$\frac{C_e}{Q_e} = \frac{1}{Q_m K_L} + \frac{C_e}{Q_m} \tag{3}$$

$$\ln Q_e = \ln K_F + \frac{1}{n} \ln C_e \tag{4}$$

where C_e (mg/L), Q_e (mg/g) and Q_m (mg/g) represent Hg(II) ions concentration at equilibrium, uptake amount of Hg(II) ions at equilibrium and the mono-layer maximum absorption of the absorbents, respectively. K_L is Langmuir constant, and K_F is Freundlich constant, and n represents the adsorption index.

Additional, the separation factor (R_L) is calculated by the following equation (McKay, 1982), which can distinguish that the adsorption is favorable or not.

$$R_L = \frac{1}{1 + C_0 K_L} \tag{5}$$

Where, the adsorption process is favorable since the R_L value is in the range of 0 to 1, the adsorption process is unfavorable since the R_L value exceeds 1.

The Langmuir and Freundlich isotherm fitting diagram are displayed in Fig. 6**(a)** and Fig. 6**(b)** Firstly, the calculated parameters are shown in **Table S1**. Compare to the Freundlich isotherm model, the R^2 value of Langmuir model is better (0.9999 greater than 0.9556). Additional, the maximum adsorption capacity of the EIP-β-CD adsorbent (the mass proportion of β-cyclodextrin, ethylene imine polymer and glutaraldehyde is 1.0:0.4:0.2) in the experiment is 351.30 mg/g, and the theoretical maximum adsorption capacity of the EIP-β-CD adsorbent is 352.11 mg/g. Both of them are almost same or errors can be ignored, so the Langmuir isotherm model could better describe the isotherm adsorption behavior using the EIP-β-CD adsorbent.

The values of the R_L ([0.0192–0.0033] less than 1) are in favorable boundary by relevant calculation, indicating that EIP-β-CD is an effective adsorbent for adsorption of Hg(II) ions in water solution.This adsorption is belonged to a monolayer adsorption with active centers (hydroxyl, amino), which is not effected by the adsorbed quantity and energetically (Elmi et al., 2020).

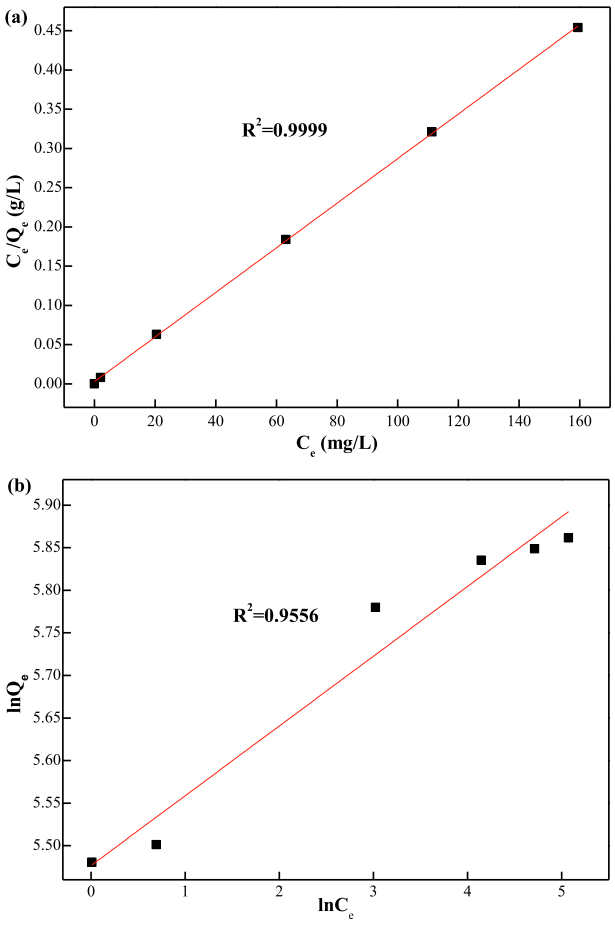

Fig. 6 (a) Langmuir isotherm plots and (b) Freundlich isotherm plots for the adsorption of Hg(II) ions.

3.5. Effect of adsorption time and adsorption kinetics analysis

3.5.1. Effect of adsorption time

The influence of the adsorption time by the EIP-β-CD adsorbent (the mass proportion of β-cyclodextrin, ethylene imine polymer and glutaraldehyde is 1.0:0.4:0.2) is shown in Fig. 7**,** and the influence of adsorption time in the adsorption experiments is different from 0 to 210 min. When the initial stage is less than 120 min, the adsorption capacity of the EIP-β-CD adsorbent increases distinctly. However, the adsorption rate (R) increases slowly and maintain the maximum value since the adsorption time exceeds 120 min. At the first step, there are many active adsorptive sites (–OH, $–NH_2$) on the surface, and Hg(II) ions could be adsorbed by these sites rapidly. Significant charge repulsion between Hg(II) ions and active adsorptive sites can be occurred, so the amount increases rapidly. Concurrently, with the decrease of the active adsorptive sites and the decline of Hg(II) ions in the solution, which are not favorable for further adsorption, so the adsorption rate decreases distinctly. The adsorption capacity almost keep the same with the adsorption time is changed from 180 to 210 min, so the adsorption reach the dynamic equilibrium state. The optimal adsorption time is 180 min, and the maximum adsorption capacity and the maximum removal rate are 248.72 mg/g and 99.49 %, respectively.

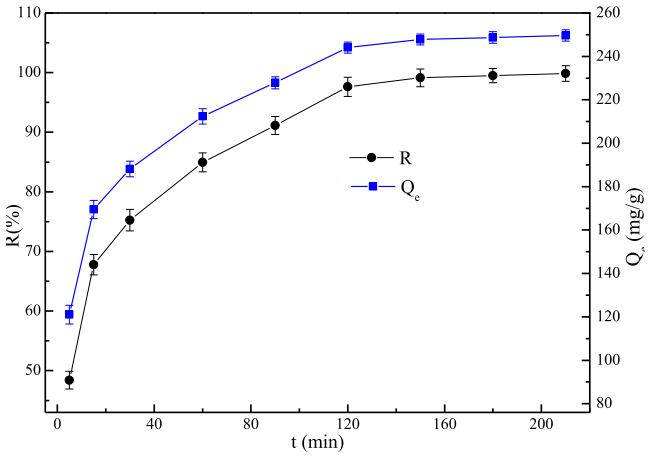

Fig. 7 Effect of adsorption time on the uptake of Hg(II) ions.

3.5.2. Kinetic analysis

The adsorption kinetics can be used for investigating the appropriate reaction rate and mechanism model. For revealing the mass transfer process, chemical reaction and control mechanism, the adsorption capacity (Q_t) are fitted by pseudo-first-order model or pseudo-second-order model with different time intervals, the calculate models are expressed in following Eqs (Ho, 2004; Ho and McKay, 1998).

$$\ln(Q_e - Q_t) = \ln Q_e - k_1 t \tag{6}$$

$$\frac{t}{Q_t} = \frac{1}{k_2 Q_{e(cal)}^2} + \frac{1}{Q_{e(cal)}} t \tag{7}$$

Where, Q_t and Q_e (mg/g) represent the adsorption capacity at time t and equilibrium time, respectively. t (min) is adsorption time, k_1 is the pseudo-first-order model rate constant, and k_2 is the pseudo-second-order model rate constant.

The kinetic curves of Hg(II) ions adsorption are displayed in Fig. 8**(a)** and Fig. 8**(b)**, and many kinetic parameters (R^2, k_1, k_2, and $Q_{e(cal)}$) are listed in **Table S2**. The determination coefficient (R^2 = 0.9971) of pseudo-second-order model is better than the determination coefficient of pseudo-first-order (R^2 = 0.9685), so the pseudo-second-order model is more suitable for describing this adsorption kinetic system. The calculated adsorption capacity $Q_{e(cal)}$ of the EIP-β-CD adsorbent (the mass proportion of β-cyclodextrin, ethylene imine polymer and glutaraldehyde is 1.0:0.4:0.2) with the pseudo-second-order kinetic model analysis is closer to the really experimental value, suggesting the removal of Hg(II) ions by this adsorbent show important feature of chemical adsorption. Electrostatic binding and chelating adsorption might are the major adsorption behaviors (Li et al., 2015).

The maximum single-layer adsorption capacity for Hg(II) ions in water solution by the different adsorbents are listed in **Table S3**. Obviously, the EIP-β-CD adsorbent (the mass proportion of β-cyclodextrin, ethylene imine polymer and glutaraldehyde is 1.0:0.4:0.2) show great advantage than many adsorbents displayed in **Table S3** (Awual et al., 2016; Girginova et al., 2010; Monier and Abdel-Latif, 2012; Naushad et al., 2015; Shi et al., 2018; Sun et al., 2021; Yang et al., 2021; Zhuo et al., 2017; Phothitontimongkol et al., 2009). Hence, the huge adsorption capacity of this adsorbent is affirmative which indicate it can be used for the removal of Hg (II) ions in water solution.

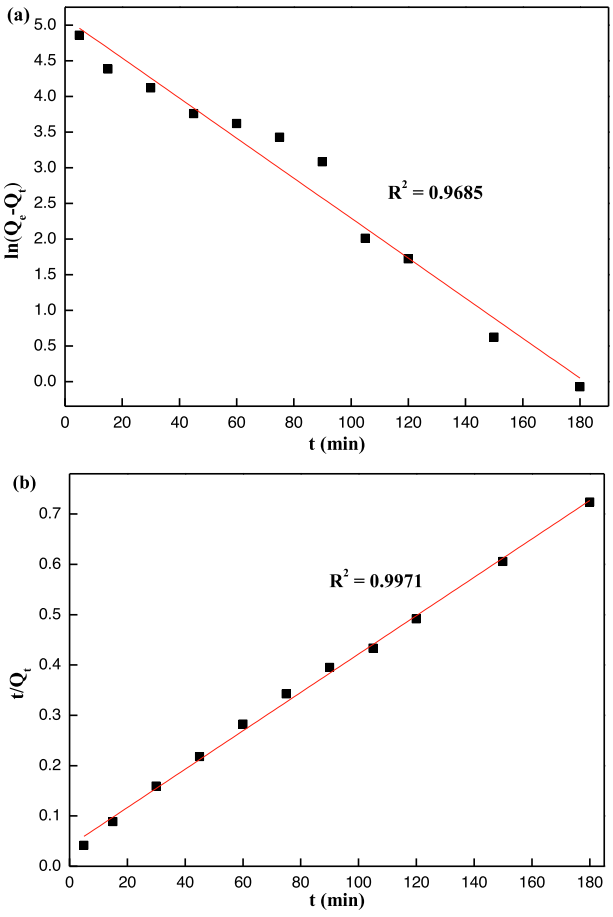

Fig. 8 Fit of kinetic data with pseudo-first-order model (a) and pseudo-second-order model (b).

3.6. Effect of the temperature and thermodynamic analysis

The adsorption Hg(II) ions experiments by this adsorbent (the mass proportion of β-cyclodextrin, ethylene imine polymer and glutaraldehyde is 1.0:0.4:0.2) are investigated at many different temperatures (from 293 to 333 K), and the variation trends are displayed in Fig. 9. The high temperature is not helpful for the adsorption of Hg(II) ions in water solution, but the adsorption rate is low at low temperature, so 293 K was the optimal temperature. Both the adsorption capacity and the removal rate for Hg(II) ions decrease distinctly with the increment of adsorption temperature, which due to the adsorbed Hg(II) ions is easier to detach the EIP-β-CD adsorbent at high temperature. Consider the hydrolysis of Hg(II) ions occur easily at high temperature, so the low temperature is more suitable to the adsorption behavior. Additional, the thermodynamic parameters are obtained by the Van terhoff equation, and ΔH^0 represents the enthalpy change, ΔS^0 represents the entropy change and ΔG^0 represents the Gibbs

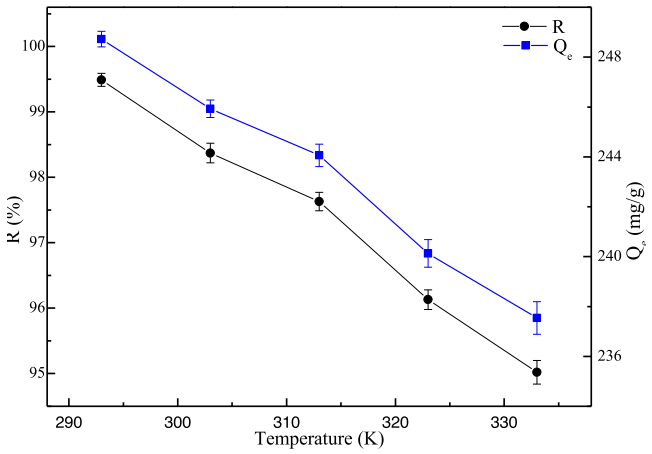

Fig. 9 Effect of adsorption temperature.

free energy change (Monier and Abdel-Latif, 2012; Yuan et al., 2020; Zhou and Zhou, 2014).

$$K_d = \frac{C_{ad}}{C_e} = \frac{C_0 - C_e}{C_e} \tag{8}$$

$$\Delta G^0 = -RTLnK_d \tag{9}$$

$$\Delta G^0 = \Delta H^0 - T\Delta S^0 \tag{10}$$

$$\ln(K_d) = \frac{\Delta S^0}{R} - \frac{\Delta H^0}{RT} \tag{11}$$

Where K_d is the equilibrium constant, C_{ad} is the concentration of solute adsorbed on the adsorbent at equilibrium (mg/L), C_0 and C_e are the initial and equilibrium concentrations of Hg(II) ions (mg/L), R is the gas constant, and T is the temperature (K). Van't Hoff plots of ln K_d against $1/T$ are drawn, and ΔH^0 and ΔS^0 are calculated from the slope (-$\Delta H^0/R$) and intercept ($\Delta S^0/R$), respectively.

According to the data analysis in **Fig.S1** and **Table S4**, All ΔG and ΔH^0 values are negative at different temperatures, so the adsorption process of Hg(II) ions by the EIP-β-CD adsorbent is spontaneous and exothermic.

3.7. Different composition of adsorbent

For investigating the effect of the composition of adsorbent, the mass of β-cyclodextrin, ethylene imine polymer and glutaraldehyde are changed carefully. So the different mass of reactants are discussed by many testing, and the results are displayed in Table 2, Table 3 **and** Table 4.

It is clear that the different mass of addition can perform the different adsorption performance. The adsorption capacity of adsorbent is developed with the increment of ethylene imine polymer in Table 2. But too much ethylene imine polymer is not ideal due to the capacity of crosslinking reagent is limited. Proper β-cyclodextrin is helpful to develop the adsorption capacity of adsorbent in Table 3, but too much β-cyclodextrin need more crosslinking reagent and the cost of adsorbent is increased. When the mass ratio between β-cyclodextrin and ethylene imine polymer is kept as 0.4:1.0, the effect of glutaraldehyde are listed in Table 4. The best optimum mass of glutaraldehyde is 0.20 g, and the crosslinking reaction only can be performed well base on the proper proportion of reactants. When the mass proportion of β-cyclodextrin, ethylene imine polymer and glutaraldehyde is 1.0:0.4:0.2, the maximum removal of Hg(II) ions is appeared as 99.49 % and the adosrption capacity of EIP-β-CD reach 248.72 mg/g. The increment mass of β-cyclodextrin or ethylene imine polymer can increase the active sites amount of adsorbent, but the mass of glutaraldehyde can effect the crosslinking density.

3.8. Effect of interfering ions

In industrial wastewater, there are many metal ions may compete with Hg(II) ions in the adsorption process at the same condition, so the competitive adsorption experiments of interfering ions need be investigated. Many coexisting cations such as Na(I), K(I), Mg(II), Ca(II) and Al(III) are mixed with the Hg(II) ions solution, respectively (interfering ions concentration, 0.01 mol/L). The different adsorption capacity of the EIP-β-CD adsorbent (the mass proportion of β-cyclodextrin, ethylene imine polymer and glutaraldehyde is 1.0:0.4:0.2) for Hg(II) ions are displayed in Fig. 10. The adsorption capacity for Hg(II) ions is almost not changed, so the competitive effect is little and ignorable. The reason of high selectivity adsorption for the Hg(II) ions may is the chelation process can occur easily. There are more empty orbits for Hg(II) ions than other metal ions, so the coordination bond between adsorbent and Hg(II) ions can be formed with chelation effect. Thereby the high selective adsorption for Hg(II) ions has been confirmed.

In order to investigate the adsorb behavior in industrial wastewater, the EIP-β-CD adsorbents (the mass proportion of β-cyclodextrin, ethylene imine polymer and glutaraldehyde

Table 2 Effect of the mass of ethylene imine polymer*.

Order	The mass of addition (g)			R (%)	Q_e (mg/g)
	β-cyclodextrin	ethylene imine polymer	glutaraldehyde		
1	1.00	0.10	0.20	64.23	160.58
2	1.00	0.20	0.20	72.17	180.43
3	1.00	0.30	0.20	90.54	226.35
4	1.00	0.40	0.20	99.49	248.72
5	1.00	0.50	0.20	99.11	247.79
6	1.00	0.60	0.20	97.47	243.68

* note: the mass of MMS-NH_2 is 0.05 g. Conditions: adsorbent 0.01 g, temperature 293 K, C_0 50 mg/L, pH 5.0, time 180 min, stirring rate 600 rpm.

Table 3 Effect of the mass of β-cyclodextrin*.

Order	The mass of addition (g)			R (%)	Q_e (mg/g)
	β-cyclodextrin	ethylene imine polymer	glutaraldehyde		
1	0.80	0.40	0.20	88.56	221.40
2	0.90	0.40	0.20	90.54	226.35
3	1.00	0.40	0.20	99.49	248.72
4	1.10	0.40	0.20	95.39	238.47
5	1.20	0.40	0.20	92.14	230.35

* note: the mass of MMS-NH_2 is 0.05 g. Conditions: adsorbent 0.01 g, temperature 293 K, C_0 50 mg/L, pH 5.0, time 180 min, stirring rate 600 rpm.

Table 4 Effect of the mass of glutaraldehyde*.

Order	The mass of addition (g)			R (%)	Q_e (mg/g)
	β-cyclodextrin	ethylene imine polymer	glutaraldehyde		
1	1.00	0.40	0.05	74.61	186.53
2	1.00	0.40	0.10	90.23	225.58
3	1.00	0.40	0.15	96.13	240.34
4	1.00	0.40	0.20	99.49	248.72
5	1.00	0.40	0.25	97.62	244.05
6	1.00	0.40	0.30	95.47	238.68

* note: the mass of MMS-NH_2 is 0.05 g. Conditions: adsorbent 0.01 g, temperature 293 K, C_0 50 mg/L, pH 5.0, time 180 min, stirring rate 600 rpm.

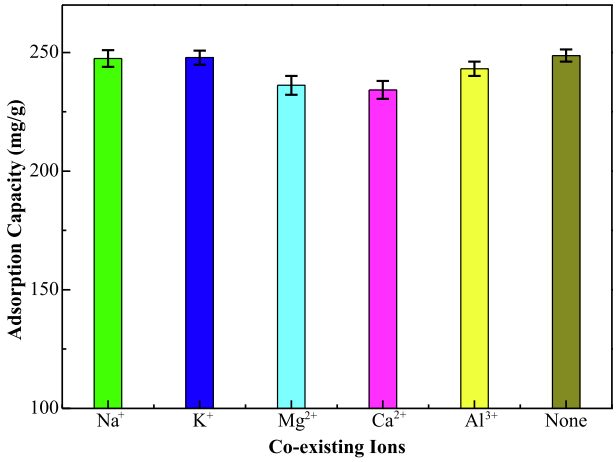

Fig. 10 The adsorption capacity of EIP-β-CD for Hg(II) ions under the coexistence ions.

is 1.0:0.4:0.2) were also used in industrial wastewater. Firstly, the industrial wasterwater (2800 mg/L) was diluted to 100 mg/L carefully, and it was used to evaluate the adsorbent's adsorbability. Adsorption time was fixed as 180 min, the mass of adsorbent was 0.02 g and pH value of solution was kept as 5.0. After adsorption process, the removal rate of Hg(II) ions was as high as 91.38 %, so it also exhibited good adsorption performance for Hg(II) ions in industrial wastewater.

3.9. Reutilization of the EIP-β-CD adsorbent.

The reutilizate performance of the EIP-β-CD adsorbent (the mass proportion of β-cyclodextrin, ethylene imine polymer and glutaraldehyde is 1.0:0.4:0.2) is very important factor to evaluate economic value and application prospects. The regeneration performances of the EIP-β-CD adsorbent were studied and the results are displayed in Fig. 11.

After the adsorption in Hg(II) ions solution, adsorbent can be transferred into eluent solution (3 mol/L HCl (Fu et al., 2021; Sun et al., 2021). It is not obvious for the downward trend of the adsorption capacity with the increment of cycle number using this EIP-β-CD adsorbent (the mass proportion of β-cyclodextrin, ethylene imine polymer and glutaraldehyde is 1.0:0.4:0.2). The removal rate of Hg(II) ions by this adsorbent is still as high as 97.48 %, and the adsorption capacity of Hg(II) ions by this adsorbent is still as high as 243.69 mg/

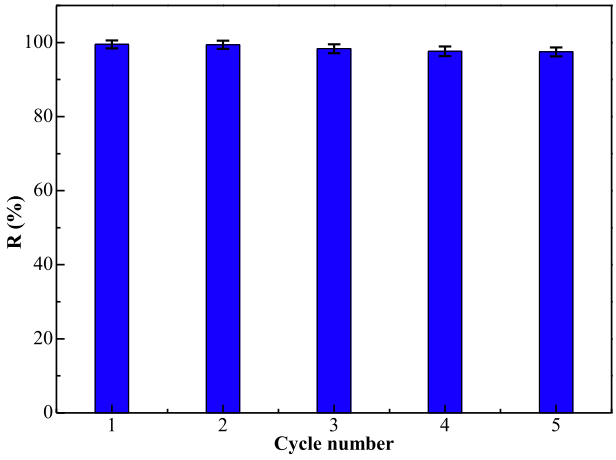

Fig. 11 Repeated use of the EIP-β-CD adsorbent.

g after 4 times of adsorption and desorption. Therefore, the good desorption capacity and good reuse capacity of this magnetic adsorbent have been certified, and it shows great application prospect.

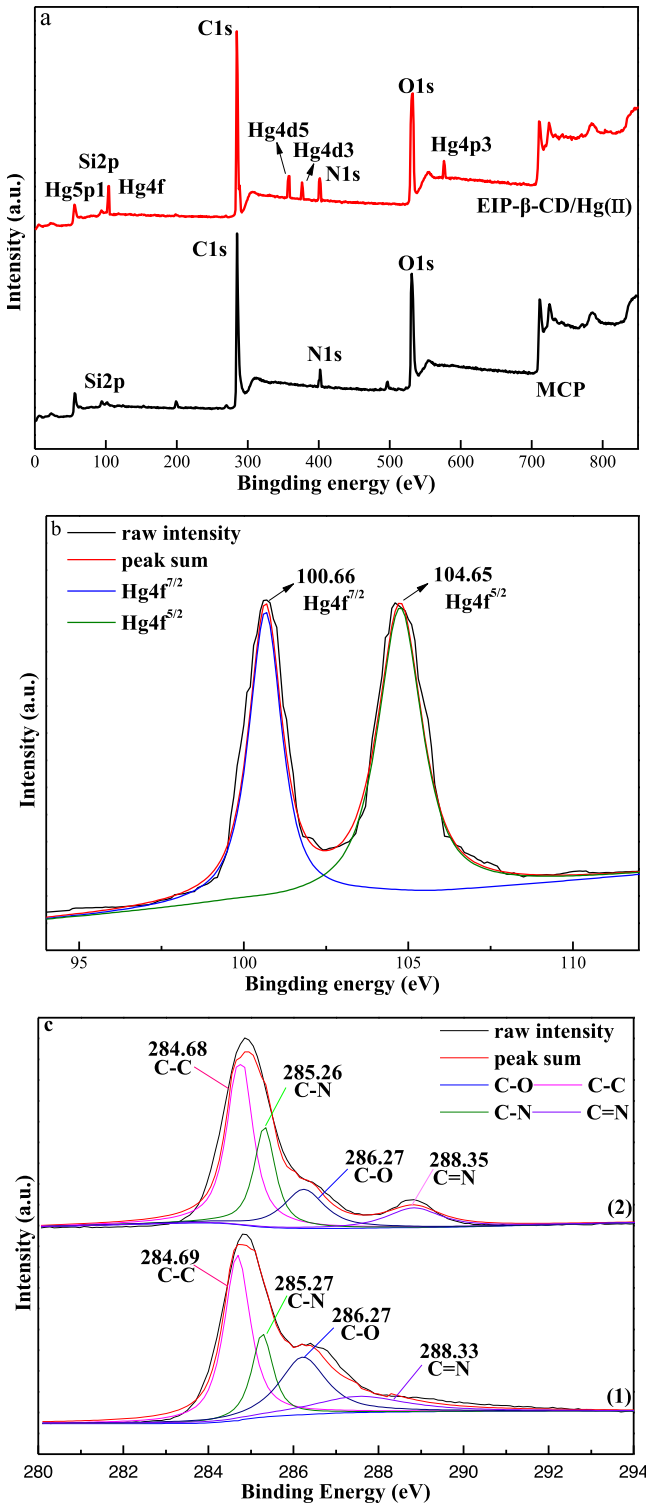

Fig. 12 (a) Full survey XPS spectra; (b) High resolution Hg 4f; (c) C1s, (d) N1s, and (e) O1s spectra of EIP-β-CD (1) fresh, (2) after adsorption.

3.10. Mechanism for adsorption of Hg(II) ions

The interaction between active groups and Hg(II) ions is investigated, both the FT-IR spectra (**Fig. S2**) and XPS characterization (Fig. 12) are used to reveal the chemical compositions of the EIP-β-CD and EIP-β-CD/Hg(II) samples. Compare to the FT-IR curve of the EIP-β-CD adsorbent, the peak near 1093 cm^{-1} is not changed in the curve of EIP-β-CD/Hg(II) sample in **Fig.S2**, so the -C—N radical on the surface of adsorbent have not been changed. Some peaks between 1661 cm^{-1} and 1091 cm^{-1} are ascribed to the different vibrations of $–NH_2$, it become weak clearly after adsorption so the amino groups participate in the adsorption Hg(II) ions in solution. The peak near 3355 cm^{-1} is belonged to the stretching vibration of hydroxyl groups in β-CD molecule, and there are some red shift to 3367 cm^{-1} and decrease phenomenon, so the hydroxyl groups in β-CD molecule participate in the adsorption of Hg(II) ions in water solution. The coordination bonds between Hg(II) ions and hydroxyl (–OH) or imino (–NH) groups are formed by chelation effect.

In order to further explore the mechanisms of adsorption, the XPS spectra (Fig. 12) of EIP-β-CD before and after Hg

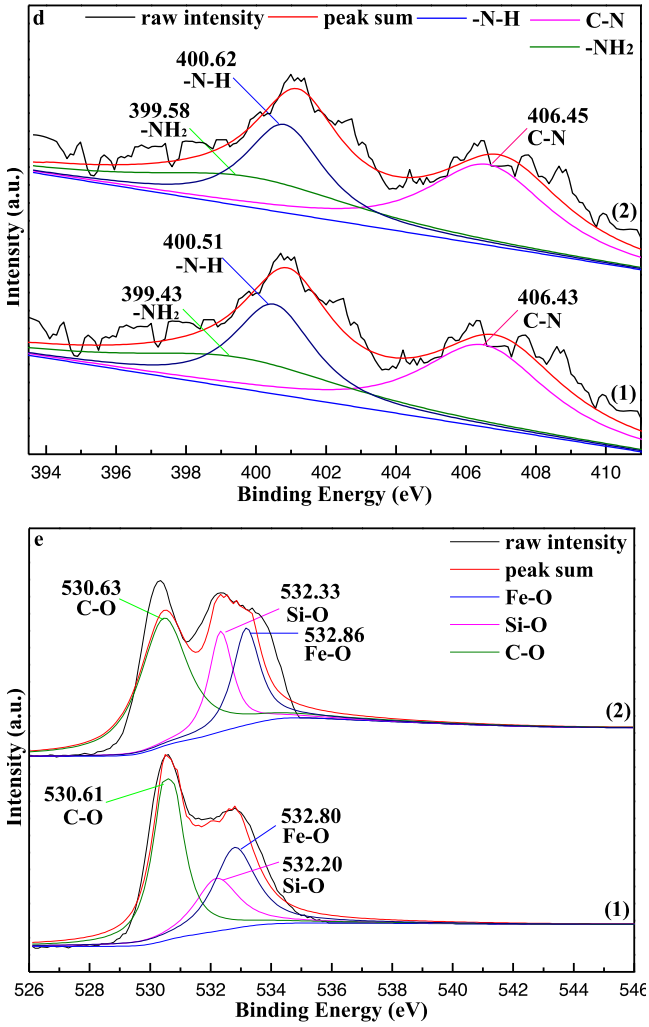

Fig. 12 (*continued*)

(II) ions adsorption are investigated. The total survey spectrums are shown in Fig. 12**(a)**, new binding energy bonds such as Hg5p1, Hg4f, Hg4d5, Hg4d3 and Hg4p3 appears in the EIP-β-CD/Hg(II) sample curve relative to the binding energies curve of the EIP-β-CD sample, so the Hg(II) ions have been adsorbed onto the surface of the EIP-β-CD adsorbent.

Two peaks at 100.66 eV and 104.65 eV (Fig. 12**(b)**) are belonged to Hg $4f^{7/2}$ and Hg $4f^{5/2}$, respectively. A binding energy gap of 3.99 eV is confirmed in the high-resolution spectra of Hg 4f, which is consist with the results in the literature (Yang et al., 2021). Additional,C1s, N1s, and O1s spectrum are recorded in Fig. 12**(c),(d) and (e)**, respectively. Some signals for the adsorption behavior of the functional groups on the surface of adsorbent are reflected in the high-resolution XPS curves.

In the deconvolution of C1s spectrum of the EIP-β-CD and EIP-β-CD/Hg(II) samples (Fig. 12**(c)**), four peaks at 284.69, 285.27, 286.27 and 288.33 eV are attributed to C—C, C—N, C—O, and C═N, respectively. Except the peaks of C—C and C═N, the intensity of the other peaks on C1s diminished are clear. Three peaks at 399.33, 400.51 and 406.43 eV in Fig. 12**(d)** represent the $–NH_2$, –NH and C—N of the adsorbent, respectively (Tian et al., 2013). The binding energy of $–NH_2$ group shifts to high binding energy (399.43–399.58) and the similar shifts for –NH group (400.51–400.62), these behaviors are ascribed to the inner influence in the adsorption process. Hence, the participation of the $–NH_2$ and –NH groups are confirmed, and which are consist with the results of FT-IR characterization results.

The O1s XPS spectra curves of the EIP-β-CD adsorbent are displayed in Fig. 12**(e)**, and three peaks at 530.61, 532.20 and 532.80 eV are belonged to C—O, Si-O and Fe-O, respectively (Shi et al., 2018; Huang et al., 2018). A small shift of the peak of C—O (530.63 eV) appears in the curve of the EIP-β-CD/Hg (II) sample, so the weak interaction between many hydroxyl groups of the β-CD molecule and Hg(II) ions are confirmed. At the same time, it is clear that the intensity of Si-O and Fe-O become stronger, the might reason is that the electrostatic attraction between O and Hg break the charge balance on the surface of the adsorbent.

The corresponding adsorption mechanism by the EIP-β-CD adsorbent is described in Fig. 13. There are four kinds of interactions including chelate reaction, physical adsorption, ion exchange or electrostatic attraction in this adsorption process (Yang et al., 2021). At first step, Hg(II) ions in water solution are fast adsorbed onto the surface of the EIP-β-CD magnetic adsorbent by the abundant surface functional groups via electrostatic attraction, so many amino ($–NH_2$) and hydroxyl (–OH) groups of adsorbent are necessary. After that, Chelation process is performed between Hg (II) ions and hydroxyl groups (–OH), amino groups ($–NH_2$) or oxygen atoms. The coordination bond can be formed

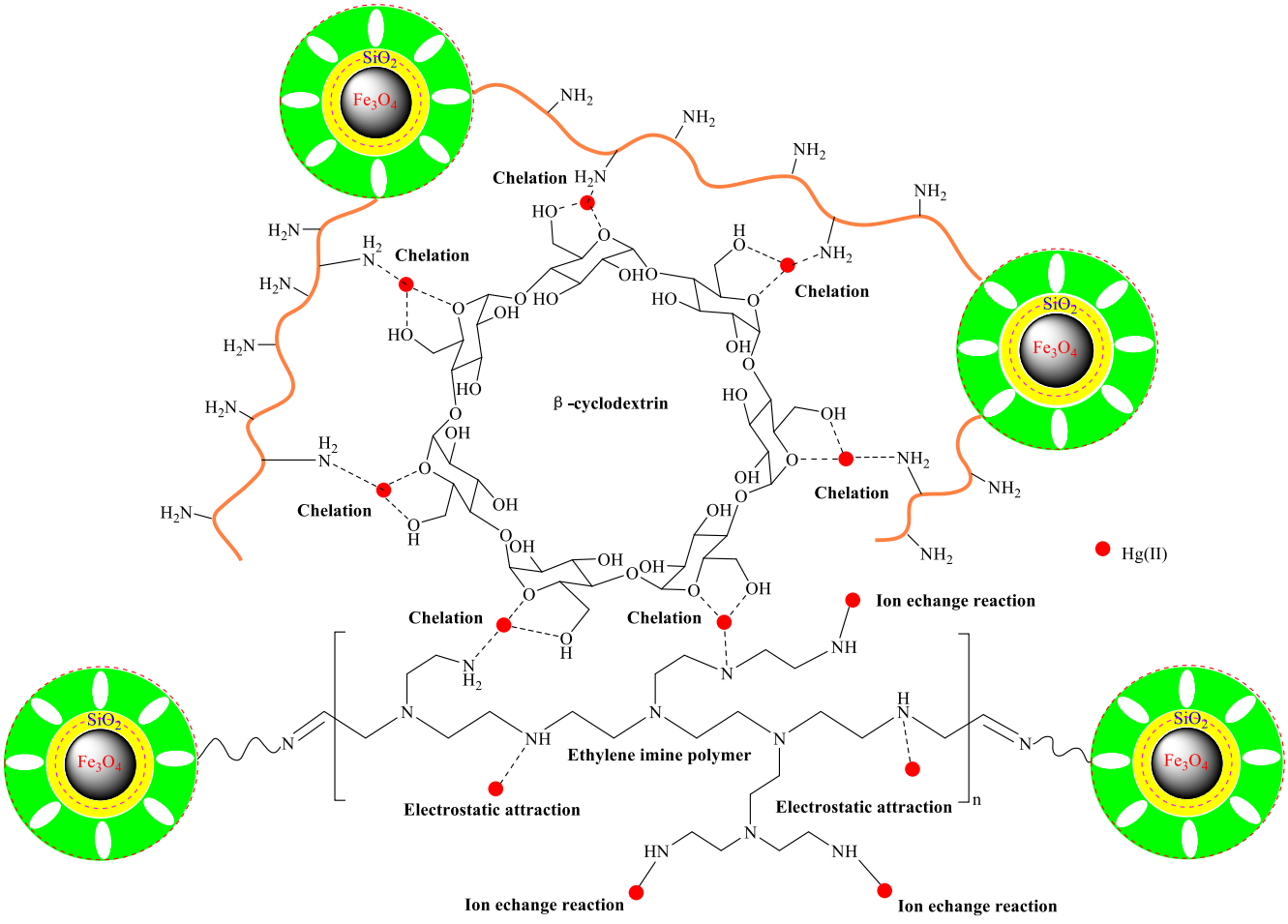

Fig. 13 The adsorption mechanism of Hg(II) ions.

easily by chelation effect, and this plays the main role in this adsorption process. At the same time, the ion exchange of the Hg(II) ions with the remnants of $-NH_2$ groups is not ignored, this behavior may improves the adsorption capacity of the EIP-β-CD adsorbent. Lastly, the migration of Hg(II) ions is inevitable, transferring from the surface of adsorbent into the nano pores of adsorbent freely, which also can improve the adsorption capacity of the EIP-β-CD adsorbent appropriately.

4. Conclusions

The EIP-β-CD adsorbent was prepared based on ethylene imine polymer/β-CD and it was used for the adsorption of Hg(II) ions in water solution. The maximum adsorption capacity of this new magnetic adsorbent was 248.72 mg/g and the correspond removal rate of Hg(II) ions reached 99.49 % under the optimized conditions. The Langmuir model was better for the adsorption isotherm analysis than Freundlich model, and the determination coefficient was as high as 0.9999, so the feature of monolayer adsorption was affirmed. This adsorption process of Hg(II) ions by the EIP-β-CD adsorbent was spontaneous and exothermic reaction by thermodynamic data analysis. The reutilization performance of this new adsorbent was good, and the adsorption capacity of this adsorbent still retained 243.69 mg/g after five recycle experiments, so the good desorption and reuse performance were affirmed and the application prospect was hugeous. The best mass proportion of β-cyclodextrin, ethylene imine polymer and glutaraldehyde was 1.0:0.4:0.2, and β-cyclodextrin could develop the adsorption capacity of adsorbent. The adsorption for Hg(II) ions by the EIP-β-CD adsorbent was independent of the interfering anions. The removal rate of Hg(II) ions in industrial wastewater by the EIP-β-CD adsorbent reached 91.38 %, so the potential capacity of this adsorbent for purify industrial wastewater was verified. All in all, these results indicated that the EIP-β-CD adsorbent was efficient and selectivity for Hg(II) ions cleanup in water solution, and it was a desirable adsorbent for Hg(II)-containing wastewater.

CRediT authorship contribution statement

Wei Long: Investigation, Writing – original draft, Resources, Funding acquisition. **Chengyue Yang:** Methodology, Investigation. **Gongshu Wang:** Methodology, Investigation. **Jianshe Hu:** Methodology, Resources, Funding acquisition, Supervision, Project administration, Writing – review & editing.

Declaration of Competing Interest

The authors declare that they have no known competing financial interests or personal relationships that could have appeared to influence the work reported in this paper.

Acknowledgements

This work was supported by Scientific Research Foundation for Fundamental Research Funds for the Central Universities (N180506002), Open Fund of Guangdong Provincial Key Laboratory of Petrochemical Pollution Process and Control, Guangdong University of Petrochemical Technology (No.2018B030322017), Projects of Talents Recruitment of GDUPT (2018rc50), and Science and Technology Plan Project of Maoming City (2019395, 2021624).

Appendix A. Supplementary material

Supplementary data to this article can be found online at https://doi.org/10.1016/j.arabjc.2022.104439.

References

Ahmadi, M., Niari, M.H., Kakavandi, B., 2017. Development of maghemite nanoparticles supported on cross-linked chitosan (γ-Fe_2O_3@CS) as a recoverable mesoporous magnetic composite for effective heavy metals removal. J. Mol. Liq. 248, 184–196. https://doi.org/10.1016/j.molliq.2017.10.014.

Awual, M.R., Hasan, M.M., Eldesoky, G.E., Khaleque, M.A., Rahman, M.M., Naushad, M., 2016. Facile mercury detection and removal from aqueous media involving ligand impregnated conjugate nanomaterials. Chem. Eng. J. 290, 243–251. https://doi.org/10.1016/j.cej.2016.01.038.

A.Z.M. Badruddoza, A.S.H. Tay, P.Y. Tan, K. Hidajat, M.S. Uddin. Carboxymethyl-β-cyclodextrin conjugat ed magnetic nanoparticles as nano-adsorbents for removal of copper ions: synthesis and adsorption studies, J. Hazard. Mater. 185 (2011) 1177-1186. https://doi.org/10.1016/j.jhazmat.2010.10.029.

Bibby, A., Mercier, L., 2002. Mercury(II) ion adsorption behavior in Thiol-functionalized mesorporous silica microspheres. Chem. Mater. 14, 1591–1597. https://doi.org/10.1021/cm0112082.

Boening, D.W., 2000. Ecological effects, transport, and fate of Mercury: a general review. Chemosphere 40, 1335–1341. https://doi.org/10.1016/S0045-6535(99)00283-0.

Chandra, V., Kim, K.S., 2011. Highly selective adsorption of Hg^{2+} by a polypyrrole-reduced graphene oxide composite. Chem. Commun. 47, 3942–3944. https://doi.org/10.1039/c1cc00005e.

Chiarle, S., Ratto, M., Rovatti, M., 2000. Mercury removal from water by ion exchange resins adsorption. Water Res. 34, 2971–2978. https://doi.org/10.1016/S0043-1354(00)00044-0.

Clercq, J.D., 2012. Removal of mercury from aqueous solutions by adsorption on a new ultra stable mesoporous adsorbent and on a commercial ion exchange resin. Int. J. Ind. Chem. 3, 1–6. https://doi.org/10.1186/2228-5547-3-1.

Dada, A.O., Olalekan, A.P., Olatunya, A.M., Dada, O., 2012. Langmuir, Freundlich, Temkin and Dubinin- Radushkevich isotherms studies of equilibrium sorption of Zn2+ unto phosphoric acid modified rice husk. IOSR J. Appl. Chem. 3, 38–45. https://doi.org/10.9790/5736-0313845.

Dziok, T., Strugala, A., Baic, I., Olszewska, D., 2020. Valorization method for hard coal as fuel for nonindustrial combustion installations with special regard to reduction of Mercury content. Energy Fuels 34, 2980–2988. https://doi.org/10.1021/acs.energyfuels.9b04267.

Elmi, F., Damghani, F.M., Taleshi, M.S., 2020. Kinetic and isotherm studies of adsorption of metribuzin herbicide on Fe_3O_4/CNT@PDA hybrid magnetic nanocomposite in wastewater. Ind. Eng. Chem. Res. 59, 9604–9610. https://doi.org/10.1021/acs.iecr.9b07077.

Forbes, E.A., 1974. The specific adsorption of inorganic Hg(II) species and Co(III) complex ions on goethite. J. Colloid Interf. Sci. 49, 403–409. https://doi.org/10.1016/0021-9797(74)90385-3.

Fu, Y., Jiang, J.W., Chen, Z.P., Ying, S.M., 2019. Rapid and selective removal of Mercury(II) ions and high catalytic performance of the spent adsorbent based on functionalized mesoporous silica/poly (m-aminothiophenol) nanocomposite. J. Mol. Liq. 286, 110746–110755. https://doi.org/10.1016/j.molliq.2019.04.023.

Fu, Y., Yang, C.Y., Zheng, Y.T., Jiang, J.W., Sun, Y., Chen, F., Hu, J. S., 2021. Sulfur corsslinked poly(m-aminothio phenol)/potato starch on mesoporous silica for efficient Hg(II) removal and reutilization of waste adsorbent as a catalyst. J. Mol. Liq. 328, 115420–115430. https://doi.org/10.1016/j.molliq.2021.115420.

Gallup, D.L., O'Rear, D.J., Radford, R., 2017. The behavior of mercury in water, alcohols, monoe thylene glycol, and triethyleneglycol. Fuel 196, 178–184. https://doi.org/10.1016/j.fuel.2017.01.100.

Gawish, S.M., Ramadan, A.M., Abo El-Ola, S.M., Abou El-Kheir, A. A., 2009. Citric acid used as a cross-linking agent for grafting β-cyclodextrin onto wool fabric. Polym-Plast. Technol. Eng. 48, 701–710. https://doi.org/10.1080/03602550902824572.

Ghasemzadeh, M.A., Abdollahi-Basir, M.H., Babaei, M., 2015. Fe_3O_4@SiO_2-NH_2 core-shell nanocomposite as an efficient and green catalyst for the multi-component synthesis of highly substituted chromeno [2,3-b] pyridines in aqueous ethanol media. Green Chem. Lett. Rev. 8, 40–49. https://doi.org/10.1080/17518253.2015.1107139.

Girginova, P.I., Daniel-da-Silva, A.L., Lopes, C.B., Figueira, P., Otero, M., Amaral, V.S., Pereira, E., Trindade, T., 2010. Silica coated magnetite particles for magnetic removal of Hg^{2+} from water. J. Colloid Interf. Sci. 345, 234–240. https://doi.org/10.1016/j.jcis.2010.01.087.

Guo, X.L., Li, M.H., Liu, A.J., Jiang, M., Niu, X.Y., Liu, X.P., 2020. Adsorption mechanisms and characteristics of Hg^{2+} removal by different fractions of biochar. Water 12, 2105–2116. https://doi.org/10.3390/w12082 105.

Ho, Y., 2004. Citation review of Lagergran kinetic rate equation on adsorption reactions. Scientometrics 59, 171–177. https://doi.org/10.1023/B:SCIE.000001330.

Ho, Y., McKay, G., 1998. A comparison of chemisorption kinetic models applied to pollutant removal on various sorbents. Process. Saf. Environ. Prot. 76, 332–340. https://doi.org/10.1205/095758298529696.

Ho, Y., Porter, J., McKay, G., 2002. Equilibrium isotherm studies for the sorption of divalent metal ions onto peat: copper, nickel and lead single component systems. Water Air Soil Pollut. 141, 1–33. https://doi.org/10.1023/A:1021304828010.

Hoti, G., Caldera, F., Cecone, C., Pedrazzo, A.R., Anceschi, A., Appleton, S.L., Monfared, Y.K., Trotta, F., 2021. Effect of the cross-linking density on the swelling and rheological behavior of ester-bridged β-cyclodextrin nanosponges. Materials 14, 478–498. https://doi.org/10.3390/ma14030478.

Q. Huang, M. Liu, J. Zhao, J. Chen, G. Zeng, H. Huang, Y. Wei. Facile preparation of polyethylenimine-tannins coated SiO_2 hybrid materials for Cu^{2+} removal, Appl. Surf. Sci. 427 (2018) 535-544, https://doi.org/10. 1016/j.apsusc.2017.08.233.

Kingston, S., 2020. The polluter pays principle in EU climate law: An effective tool before the courts? Climate Law 10 (1), 1–27. https://doi.org/10.2139/ssrn.3680025.

Li, Q., Sun, L., Zhang, Y., Qian, Y., Zhai, J.P., 2011. Characteristics of equilibrium, kinetics studies for adsorption of Hg(II) and Cr(VI) by polyaniline/humic acid composite. Desalination 266, 188–194. https://doi.org/10.1016/j.desal.2010.08.025.

Li, X., Zhou, H., Wu, W., Wei, S., Xu, Y., Kuang, Y., 2015. Studies of heavy metal ion adsorption on Chitosan/ Sulfydryl-functionalized graphene oxide composites. J. Colloid. Interf. Sci. 448, 389–397. https://doi.org/10.1016/j.jcis.2015.02.039.

Ma, X.J., Li, Y.F., Ye, Z.F., Yang, L.Q., Zhou, L.C., Wang, L.Y., 2011. Novel chelating resin with cyanoguanidine group: useful recyclable materials for Hg(II) removal in aqueous environment. J. Hazard. Mater. 185, 1348–1356. https://doi.org/10.1016/j.jhazmat.2010.10.054.

G, McKay. Adsorption of dyestuffs from aqueous solutions with activated carbon I: Equilibrium and batch contact-time studies. J. Chem. Technol. Biotechnol. 32 (1982) 759-772. http://dx.doi.org/10.1002/jctb.5030 320712.

B.B. Mo, B. Lian. Hg(II) adsorption by Bacillus mucilaginosus: mechanism and equilibrium parameters, World J Microbiol Biotechnol. 27 (2010) 1063-1070, https://doi.org/10.1007/s11274-010-0551-z.

Mohamed, M.H., Wilson, L.D., Pratt, D.Y., Guo, R., Wu, C., Headley, J.V., 2012. Evaluation of the accessible inclusion sites in copolymer materials containing beta-cyclodextrin. Carbohyd. Polym. 87, 1241–1248. https://doi.org/10.1016/j.carbpol.2011.09.011.

Monier, M., Abdel-Latif, D.A., 2012. Preparation of cross-linked magnetic chitosan-phenylthiourea resin for adsorption of Hg(II), Cd(II) and Zn(II) ions from aqueous solutions. J. Hazard. Mater. 209–210, 240–249. https://doi.org/10.1016/j.jhazmat.2012.01.015.

Monrin-Crini, N., Crini, G., 2013. Environmental applications of water-insoluble β-cyclodextrin-epichlorohydrin polymers. Prog. Polym. Sci. 38, 344–368. https://doi.org/10.1016/j.progpolymsci.2012. 06.005.

Naushad, M., Vasudevan, S., Sharma, G., Kumar, A., Alothman, Z. A., 2015. Adsorption kinetics, isotherms, and thermodynamic studies for Hg^{2+} adsorption from aqueous medium using alizarin red-S-loaded amberlite IRA-400 resin. Desalin. Water Treat. 57, 1–9. https://doi.org/10.1080/19443994.2015.1090914.

Park, J.H., Wang, J.J., Xiao, R., Pensky, S.M., Kongchum, M., DeLaune, R.D., Seo, D.C., 2018. Mercury adsorption in the mississippi river deltaic plain freshwater marsh soil of louisiana gulf coastal wetlands. Chemosphere 195, 455–462. https://doi.org/10.1016/j.chemosphere.2017.12.104.

T. Phothitontimongkol, N. Siebers, N. Sukpirom, F. Unob. Preparation and characterization of novel organo-clay minerals for Hg(II) ions adsorption from aqueous solution. Appl. Clay Sci. 43 (2009) 343-349. https://doi.org/10.1016/j.clay.2008.09.016.

P.D. Pigatto, A. Costa, G. Guzzi, Are mercury and Alzheimer's disease linked? Sci. Total Environ. 613-614 (20 18) 1579-1580, https://doi.org/10.1016/j.scitotenv.2017.09.036.

Pourshirband, A., Nezamzadeh-Ejhieh, A., 2020. Experimental design on determination of Sn(II) by the modified carbon paste electrode with Fe-exchanged clinoptilolite nanoparticles. Soild State. Sci. 99 (1060), 82–106091. https://doi.org/10.1016/j.solidstatesciences.2019.106082.

Pouya, G.K., Bagherzade, G., Eshghi, H., 2020. Design and synthesis of magnetic Fe_3O_4@NFC-ImSalophCu nanocatalyst based on cellulose nanofibers as a new and highly efficient, reusable, stable and green catalyst for the synthesis of 1,2,3-trazoles. RSC Adv. 10, 32927–32937. https://doi.org/10.1039/D0RA06251K.

Rivas, B.L., Urbano, B., Pooley, S.A., Bustos, I., Escalona, N., 2012. Mercury and lead sorption properties of poly(ethyleneimine) coated onto silica gel. Polym. Bull. 68, 1577–1583. https://doi.org/10.1007/s00289-011-0636 -3.

Saeed, M.M., Hasany, S.M., Ahmed, M., 1999. Adsorption and thermodynamic characteristics of Hg(II)-SCN complex onto polyurethane foam. Talanta 50, 625–634. https://doi.org/10.1016/S0039-9140(99)00158 -7.

She, M., Jia, C.Q., Duan, Y., Zhu, C., 2020. Influence of different sulfur forms on gas-phase Mercury removal by S_O2-Impregnated porous carbons. Energy Fuels 34, 2064–2072. https://doi.org/10.1021/acs.Energy fuels.9b03648.

Shi, Z.N., Xu, C., Lu, P., Fan, L., Li, L., 2018. Preparation and the adsorption ability of thiolated magnetic core-shell Fe_3O_4@SiO_2@-C-SH for removing Hg^{2+} in water solution. Mater. Lett. 225, 130–133. https://doi.org/10.1016/j.matlet.2018.04.098.

Somayajula, A., Aziz, A.A., Saravanan, P., Matheswaran, M., 2013. Adsorption of mercury(II) ion from aqueous solution using low-cost activated carbon prepared form mango kernel. Asia-Pac. J. Chem. Eng. 8, 1–10. https://doi.org/10.1002/apj.1613.

Sun, Y., Wu, Y., Fu, Y., Yang, C.Y., Jiang, J.W., Yan, G.Y., Hu, J.S., 2021. Rapid and high selective removal of Hg(II) ions using tannic acid cross-linking cellulose/ethylene imine polymer functionalized magnetic composite. Int. J. Biol. Macromol. 182, 1120–1129. https://doi.org/10.1016/j.ijbiomac.2021.04.091.

Szejtli, J., 1998. Introduction and general overview of cyclodextrin chemistry. Chem. Rev. 98, 1743–1754. https://doi.org/10.1021/cr970022c.

Tian, Y., Wu, M., Liu, R.G., Li, Y.X., Wang, D.Q., Tan, J.J., Wu, R. C., Huang, Y., 2011. Electrospun membrane of cellulose acetate for

heavy metal ions adsorption in water treatment. Carbohyd. Polym. 83, 743–751. https://doi.org/10.1016/j.carbpol.2010.08.054.

Tian, Y., Cao, Y., Wang, Y., Yang, W., Feng, J., 2013. Realizing ultrahigh modulus and high strength of macroscopic graphene oxide papers through crosslinking of mussel-inspired polymer. Adv. Mater. 25, 2980–2983. https://doi.org/10.1002/adma.201300118.

I. Ullah, L.H. Zhao, Y. Hai, M. Fahim, D. Alwayli, X. Wang, H.Y. Li. Metal elements and pesticides as risk factors for parkinson's disease - A review. Toxicol Rep. 10 (4) (2021) 607-616, https://doi.org/10.1016/j. toxrep. 2021.03.009. eCollection 2021.

X.H. Wang, L. Yang, J.P. Zhang, C.Y. Wang, Q.Y. Li. Preparation and characterization of chitosan-poly(vinyl alcohol)/bentonite nanocomposites for adsorption of Hg(II) ions, Chem. Eng. J. 251 (2014) 404-412, https: //doi.org/ 10.1016/j.cej.2014.04.089.

Wang, T., Wu, J.W., Zhang, Y.S., Liu, J., Sui, Z.F., Zhang, H.C., Chen, W.Y., Norris, P., Pan, W.P., 2018. Increasing the chlorine active sites in the micropores of biochar for improved mercury adsorption. Fuel 229, 60–67. https://doi.org/10.1016/j.fuel.2018.05.028.

Weber, W.J., Morris, J.C., 1963. Kinetics of adsorption on carbon from solution. J. Sanit. Eng. Div. 89, 31–60.

Yan, J., Zhu, Y., Qiu, F.X., Zhao, H., Yang, D.Y., Wang, J., Wen, W. Y., 2016. Kinetic, isotherm and thermodynamic studies for removal of methyl orange using a novel β-cyclodextrin functionalized graphene oxide-isophorone diisocyanate composites. Chem. Eng. Res. Des. 106, 168–177. https://doi.org/10.1016/j.cherd.2015.12.023.

Yang, J.S., Han, S.Y., Yang, L., Zheng, H.C., 2016. Synthesis of beta-cyclodextrin-grafted-alginate and its application for removing methylene blue from water solution. J. Chem. Technol. Biot. 91, 618–623. https://doi.org/10.1002/jctb.4612.

Yang, C.Y., Jiang, J.W., Wu, Y., Fu, Y., Sun, Y., Chen, F., Yan, G. Y., Hu, J.S., 2021. High removal rate and selectivity of Hg(II) ions using the magnetic composite adsorbent based on starch/ethylene imine polymer. J. Mol. Liq. 337, 116418–116429. https://doi.org/10.1016/j.molliq.2021.116418.

Yilmaz, S., Sahan, T., Karabakan, A., 2017. Response surface approach ofr optimization of Hg(II) adsorption by 3-mercapto-propyl trimethoxysilane-modified kaolin minerals from aqueous solution. Korean J. Chem. Eng. 11, 2225–2235. https://doi.org/10.1007/s11814-017-0116-z.

Yuan, Q., Chi, Y., Yu, N., Zhao, Y., Yan, W., Li, X., Dong, B., 2014. Amino-functionalized magnetic mesoporous microspheres with good adsorption properties. Mater. Res. Bull. 49, 279–284. https://doi.org/10.1016/j.materresbull.2013.08.063.

Yuan, Z.Y., Liu, H.Q., Wu, H.X., Wang, Y.M., Liu, Q., Wang, Y., Lincoln, S.F., Guo, X.H., Wang, J., 2020. Cyclodextrin hydrogels: rapid removal of aromatic micropollutants and adsorption mechanisms. J. Chem. Eng. Data 65, 678–689. https://doi.org/10.1021/acs.jced.9b00913.

Zhang, Y., Qu, R.J., Sun, C.M., Wang, C.H., Ji, C.N., Chen, H., Yin, P., 2009. Chemical modification of silica-gel with diethylenetriamine via an end-group protection approach for adsorption to Hg (II). App. Surf. Sci. 255, 5818–5826. https://doi.org/10.1016/j.apsusc.2009.01.011.

J. Zhou, Y. Li, L. Sun, Z. Tang, L. Qi, L. Liu, Q. Liang. Porous silica-encapsulated and magnetically recover able Rh NPs: a highly efficient, stable and green catalyst for catalytic transfer hydrogenation with "slow-release" of stoichiometric hydrazine in water, Green Chem. 19 (2017) 3400-3407, https://doi.org/10. 1039/C7GC00986K.

Zhou, L.M., Wang, Y.P., Liu, Z.R., Huang, Q.W., 2009. Characteristics of equilibrium, kinetics studies for adsorption of Hg(II), Cu (II) and Ni(II) ions by thiourea-modified magnetic chitosan microspheres. J. Hazard. Mater. 161, 995–1002. https://doi.org/10.1016/j.jhazmat.2008.04.078.

Zhou, L.M., Liu, Z.R., Liu, J.H., Huang, Q.W., 2010. Adsorption of Hg(II) from aqueous solution by ethylenediamine- modified magnetic crosslinking chitosan microspheres. Desalination 258, 41–47. https://doi.org/10.1016/j.desal.2010.03.051.

Zhou, X., Zhou, X., 2014. The unit problem in the thermodynamic calculation of adsorption using the Langmuir equation. Chem. Eng. Comm. 201, 1459–1467. https://doi.org/10.1080/00986445.2013.818541.

Zhuo, W.Q., Xu, H.U., Huang, R.S., Jie, Z., Xiang, Z., 2017. A Chelating polymer resin: slynthesis, characterization, adsorption and desorption performance for removal of Hg(II) from aqueous solution. Iran. Chem. Soc. 14, 2557–2566. https://doi.org/10.1007/s13738-017-1190-1.